THE JOURNAL OF PHYSICAL CHEMISTRY C

Article

pubs.acs.org/JPCC

Size-Dependent Validity Bounds on the Universal Plasmon Ruler for Metal Nanostructure Dimers

Xue Ben and Harold S. Park*

Department of Mechanical Engineering, Boston University, Boston, Massachusetts 02215, United States

ABSTRACT: We study the validity of the recently proposed universal plasmon ruler in the present work using a combination of numerical techniques based on the finite difference time domain (FDTD) method, and semianalytical theories based on the coupled dipole approximation. By incorporating nonlocal effects for closely spaced two-dimensional gold nanocylinder dimers, we find using both the FDTD and semianalytical approaches that the universal plasmon ruler of Jain et al.[1] is not applicable for gold nanocylinder dimers with diameters smaller than about 20 nm. The nonlocal effects are also found to strongly reduce the electric field enhancements at very small gap distances. Taken together with previous results,[2] we are able to establish the valid size range for the universal plasmon ruler of gold: 20 nm diameter metal nanostructure dimers at the smaller end, and 70 nm diameter metal nanostructure dimers at the larger end.

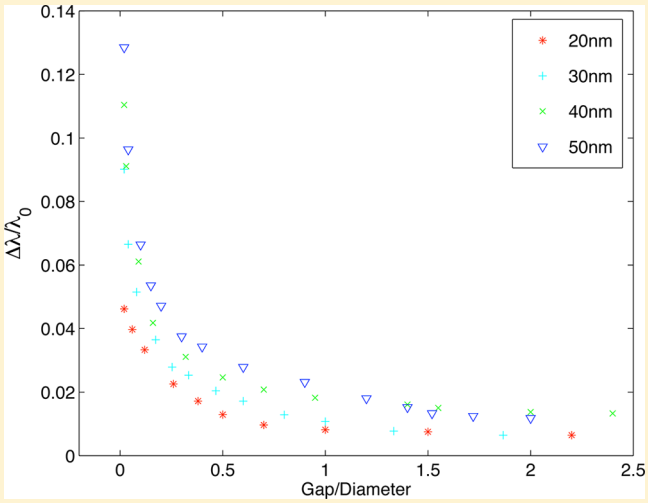

INTRODUCTION

Upon interaction with incident electromagnetic waves such as light, face-centered cubic (FCC) metal (such as gold and silver, the former being the focus of this work) nanostructures exhibit a unique optical response known as a localized surface plasmon resonance (LSPR).[3−5] Excitation of the metal nanostructure at its LSPR wavelength results in both an enhancement of the electromagnetic fields close to the surface of the nanostructure[6−8] and also an impact on the far field optical properties through absorption and scattering of the incident light.[9−11] There exists a diverse range of potential applications for plasmon resonance metal nanostructures, including optical sensing, detection and imaging[12−16] and photothermal cancer therapies,[17−19] among many others.

However, some of the most exciting applications of plasmon resonance metal nanostructures involve not an individual nanoparticle, but the interactions of two nanoparticles, a nanoparticle dimer.[7,20−28] This has recently become important primarily due to the fact that it is now experimentally possible to, either through synthesis[29] or manipulation of the existing particles,[30] control the distance separation between them.

The first important issue this opens up is the fact that the enhancement in electromagnetic fields that can occur at nanometer separations between individual nanoparticles can result in large Raman enhancements of up to 10^{12}, which would enable single molecule sensing and detection.[6,31,32]

Second, researchers have recently discovered that the distances in biological systems can be determined based on the change in the optical properties, and specifically the LSPR wavelength, that result from the interaction of two metal nanoparticles if the nanoparticle size is known.[33,34] This information is critical in order to systematically optimize the arrangements of nanoparticles with predictable and repeatable optical properties for optical sensing applications. Specifically, Sonnichsen et al.[33] and Reinhard et al.[34] called this distance-dependent relation a "plasmon ruler". The plasmon ruler was given an analytic form for the case of gold nanodisk dimers by Jain et al.,[1] who also found a nearly universal scaling of the decay length of the interactions between nanoparticle dimers that was apparently independent of nanoparticle size, shape, metal type and dielectric constant. This plasmon ruler equation was then used to explain the experimental results of Reinhard et al.[34] More recently, Ben and Park[2] determined that, for both dimers and two-dimensional arrays of gold nanoparticles, the plasmon ruler exhibited a dynamic depolarization-induced size dependence for nanoparticles larger than about 70 nm.

However, the behavior of the plasmon ruler has not been established if the distance separating nanoparticles becomes less than about 10 nm. This is because, at such small separations, classical electrodynamics may become invalid, thus necessitating the use of other physical models. One such model is the so-called nonlocal model,[35,36] which has recently been utilized both theoretically[37−42] and experimentally[43,44] to interpret the unusual blue shifts and plasmon broadening observed in the optical properties of either individual or small clusters of very small diameter or closely separated metal nanoparticles, though

Received: June 3, 2012
Revised: August 14, 2012
Published: August 15, 2012

nonlocal effects on the plasmon ruler have not been studied to date. We note the recent experimental study of Yang et al.,[45] who studied the plasmon ruler for silver nanoparticles 40 nm in diameter for separations ranging from 1 to 25 nm. The experimental results did show two clear regimes of the plasmon ruler. Of particular relevance to the present work, a deviation from the plasmon ruler was found for center-to-center distance (L) to diameter (D) ratios smaller than about 1.05. Qualitative agreement with the nonlocal results of Garcia de Abajo[38] were noted within this size range, though a direct comparison to the present results cannot be made as gold was the plasmonic material of choice in the present work.

Therefore, there exist critical unresolved issues not only as to whether the universal plasmon ruler is still valid at very small gap distances between nanoparticles but also as to the precise nanoparticles sizes for which it is valid. We study these issues in the present work using a two-dimensional nonlocal, finite difference time domain (FDTD) formulation of McMahon et al.,[37,39] and interpret the FDTD results within the context of a semianalytical theory based on the coupled dipole approximation (CDA).

NONLOCAL THEORY AND NUMERICAL METHODOLOGY

The optical response of small metal nanostructures is often modeled using the bulk Drude plus Lorentz pole(s) model, in which the Drude term describes the free electrons in the conduction band as negative charges moving collectively in an infinite homogeneous medium.[46] However, for small metallic nanostructures, particularly particles with sharp edges or interacting particles separated by very small distances, the bulk Drude model loses validity as there is no confinement or wall felt by the free electrons,[47] and the effects of spatial dispersion (or wave vector dependence) of the optical response are not captured.

One approach to incorporating these nonbulk effects is to utilize a nonlocal dielectric function, where nonlocality means that the material polarization at a point in space depends not just on the local electric field but also on the electric field in the surrounding neighborhood.[39] The result of this is that the dielectric function is not only temporally but also spatially dispersive, which leads to an additional dependence on the wavevector $\mathbf{k}$ along with the traditional dependence on frequency ω.

Formally, the motion of the free electron gas corrected by nonlocal effects is captured using the hydrodynamic equation of motion.[48] The resulting dielectric function ε_{HD} that emerges is

$$\varepsilon_{HD}(\mathbf{k}, \omega) = -\frac{{\omega_D}^2}{\omega(\omega + i\gamma) - \beta^2\mathbf{k}^2} \quad (1)$$

where ω_D is the plasmon frequency, γ is the collision frequency, and $\beta^2 = 3{v_F}^2/4$ for a two-dimensional free-electron gas at high frequencies.

We utilize the nonlocal FDTD formulation and code of McMahon et al.[37] to numerically solve Maxwell's equations, where the nonlocal and standard (local) FDTD algorithms[49] are essentially identical. The only difference in the nonlocal approach is that there is an additional material property dependence on the wavevector $\mathbf{k}$ from the hydrodynamic Drude term ε_{HD} in eq 1, i.e.,

$$\varepsilon(\mathbf{k}, \omega) = \varepsilon_\infty + \varepsilon_{Lorentz}(\omega) + \varepsilon_{HD}(\mathbf{k}, \omega) \quad (2)$$

where

$$\varepsilon_{Lorentz}(\omega) = \frac{\Delta\varepsilon_L {\omega_L}^2}{{\omega_L}^2 - \omega(\omega + i2\delta_L)} \quad (3)$$

and where ω_L is the frequency at which the d- to sp-band transition happens, $\Delta\varepsilon_L$ is the relative permittivity shift at the transition, and δ_L is the electron dephasing rate. Here, a Drude plus two Lorentz poles model was used to fit the experimental data,[39] with $\varepsilon_\infty = 3.559$, $\omega_D = 8.812$ eV, $\gamma = 0.0752$ eV, $\omega_{L1} = 4.693$ eV, $\omega_{L2} = 3.112$ eV, $\Delta\varepsilon_{L1} = 2.912$, $\Delta\varepsilon_{L2} = 1.272$, $\delta_{L1} = 1.541$ eV, $\delta_{L2} = 0.525$ eV. We note that γ is taken to be size-independent, meaning that electron-surface scattering effects, which appear to be important only for nanoparticle sizes smaller than about 5−10 nm,[50] were not accounted for as the smallest diameter cylinder we considered was 20 nm. We also note that quantum mechanical effects, such as electron spill out and quantum tunneling, are not captured in our model. A summary of other effects that a spatially nonlocal dielectric function does not capture are summarized by McMahon et al.[39]

NUMERICAL RESULTS

We performed two-dimensional FDTD simulations using both local and nonlocal formulations on a pair of infinitely long cylindrical wires that form a dimer separated by varying gap distances. Specifically, the diameters D of the cylinders ranged from 20 to 50 nm, while the corresponding gap (edge-to-edge) distances T ranged from $0.02D$ to $3D$. Because the smallest gap distance of $0.02D$ is considerably smaller compared to previous studies of plasmon rulers,[1,2] nonlocal effects are expected to be important. The dimer systems are excited in the FDTD simulations by a pulse with electric field parallel to the dimer axis and the wave vector perpendicular to the dimer axis.

Because the gap distances we have considered in our study are very small, a convergence study on the spatial grid size was performed. In doing so, we determined that, for the 20 nm diameter dimers, a mesh size of 0.1 nm was sufficient; a 0.2 nm mesh size was sufficient for the 30 and 40 nm diameter dimers, while a 0.25 nm mesh size was sufficient for the 50 nm diameter dimer.

The effects of accounting for nonlocal effects are illustrated in Figure 1, which shows the extinction profiles for 50 nm

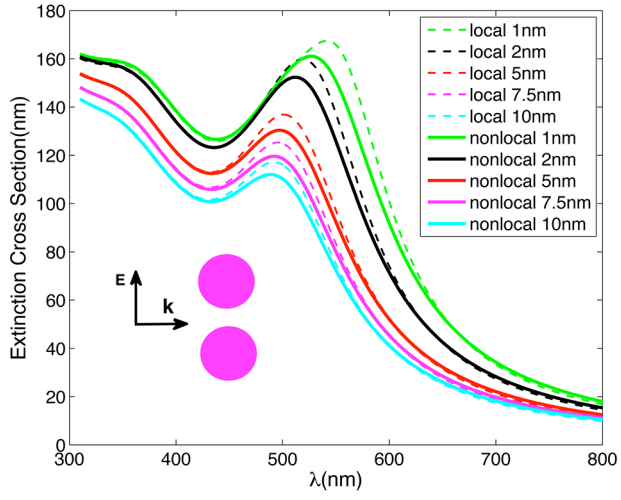

Figure 1. FDTD results of the extinction efficiency profile for 50 nm diameter cylinder dimers with gap distances ranging from 1 to 10 nm.

dx.doi.org/10.1021/jp3054372 | J. Phys. Chem. C 2012, 116, 18944−18951

cylinder diameters separated by gap distances ranging from 1 to 10 nm. There are several general trends to note. First, compared to the local resonance wavelength for a given gap distance, there is a blue shift in the corresponding nonlocal wavelength, with the blue shift becoming stronger for smaller gap distances (and also smaller diameters). This demonstrates, as has previously been found,[38,39] that nonlocal effects become stronger for smaller dimensions and separations, which can be explained by examining the hydrodynamic Drude term in the nonlocal permittivity $\varepsilon(\mathbf{k},\omega)$. Specifically, if we reduce the edge-to-edge distance separating the dimer, highly evanescent fields with larger magnitudes of $\mathbf{k}$ are generated, which implies that a higher frequency is needed to excite the localized plasmon resonance.[40] Second, we note that in general the nonlocal resonance peaks become broader and weaker as compared to the local peaks for the same diameter and gap spacing.

Before moving forward to discuss the numerical results, we note that because we have considered a two-dimensional geometry as compared to the three-dimensional plasmon ruler established by Jain et al.,[1] within the quasistatic approximation we find a $1/(T/D)^2$ dependence between the scaled plasmon shifts vs scaled gap size as compared to the $1/(T/D)^3$ dependence found for the universal plasmon ruler. The net effect is that the decay constant we obtain for the two-dimensional, infinitely long cylindrical wires are slightly different from full three-dimensional case.

We show in Figure 2 a comparison between the scaled plasmon resonance wavelength shift $(\Delta\lambda/\lambda_0)$ vs the gap/diameter ratio (T/D) for the 20−50 nm diameter cylinder dimers as calculated using both the local and nonlocal FDTD simulations. The plasmon ruler is defined as follows to describe the relationship between $\Delta\lambda/\lambda_0$ and T/D as, where λ_0 is the resonance wavelength for a single nanocylinder, D is the cylinder diameter and T is the edge-to-edge gap distance,[1]

$$\frac{\Delta\lambda}{\lambda_0} = a\, e^{-x/\tau} \tag{4}$$

where $x = T/D$ and $\Delta\lambda$ is the plasmon resonance wavelength shift compared to the individual nanocylinder resonance wavelength. It is seen in Figure 2a that, using the local theory, the curves for all cylinder dimer sizes we have considered appear to follow the same trend, particularly when the gap/diameter ratio is small. This fact is important as the exponential form of the plasmon ruler in eq 4 is designed to capture the scaled plasmon resonance shift at small gap/distance ratios.

In contrast for the nonlocal case in Figure 2b, while the 30−50 nm diameter dimers appear to follow the same scaled resonance wavelength behavior at small gap/distance ratios, there is a clear deviation for the 20 nm diameter dimers, and thus we conclude that it is at this diameter that the nonlocal effects become important. Specifically, for the smallest separations, the scaled wavelength shift $\Delta\lambda/\lambda_0$ is around 0.09 for the local dimer while decreasing substantially to about 0.05 for nonlocal one.

This fact is reinforced by comparing the plasmon rulers for the local and nonlocal cases shown in Figure 3. As can be seen in Figure 3a for the local case, the curves can be fitted to the universal plasmon ruler in eq 4, where the coupling strength $a = 0.112 \pm 0.110$, and the decay constant $\tau = 0.19 \pm 0.04$. In contrast for the nonlocal case, the 30−50 nm diameter dimers can be fit to the same universal plasmon ruler, though the coupling strength is smaller, $a = 0.098 \pm 0.01$, than the local case while the decay constant is larger, i.e., $\tau = 0.28 \pm 0.07$. The plasmon ruler for dimers with nonlocal effects is found to have a larger decay constant, which is due to the wavevector dependence of the hydrodynamic Drude term in eq 1. Further insights into the plasmon ruler will be obtained using a semianalytical model in the next section.

We close our discussion of nonlocal effects on the optical properties of cylindrical dimers by discussing the impact on the electric field enhancements. The enhancements, as calculated from the FDTD simulations, are shown in Figure 4, where the $|E|^2$ enhancement was calculated from the maximum value at the cylinder−air interface for T/D varying from 0.02 to 0.4. As seen in Figure 4a for the local dimers at constant $T/D = 0.02$, the $|E|^2$ enhancements are about 347, 476, 726, 905 respectively for 20, 30, 40, and 50 nm dimers. In contrast for the nonlocal dimers, the corresponding $|E|^2$ enhancements at constant $T/D = 0.02$ are 157, 252, 378, 496, which means that $|E|^2$ enhancements are reduced by 47.1%, 47.9%, and 45.2% for the 30, 40, and 50 nm dimers, respectively. Finally, the $|E|^2$ enhancement was reduced the most (54.6%) for the 20 nm dimer.

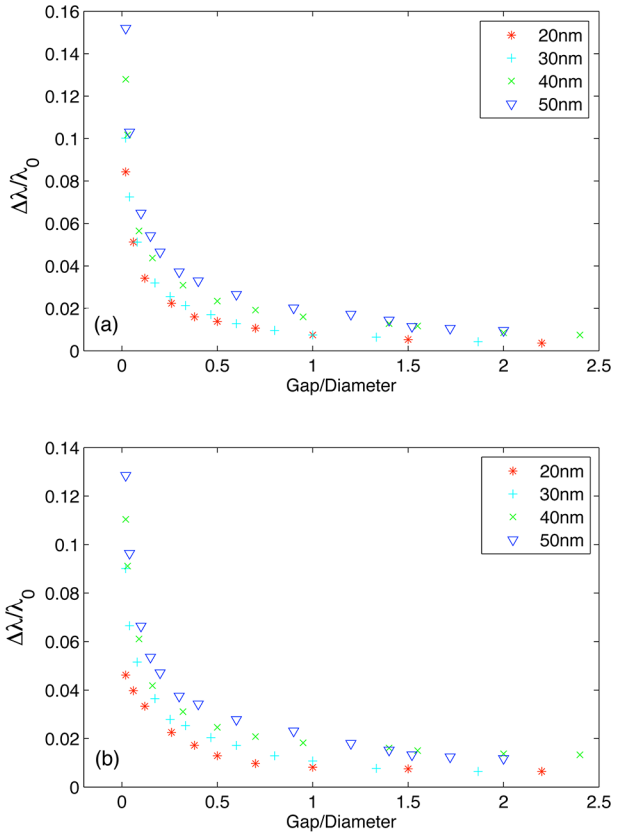

Figure 2. FDTD calculations of LSPR wavelength shift vs gap distance for 20−50 nm diameter cylinder dimers in both (a) local and (b) nonlocal responses.

SEMIANALYTICAL MODEL

To assist in interpreting the results of the nonlocal FDTD simulations, we present a semianalytical model based upon the coupled dipole approximation (CDA)[2,51] and effective permittivity (EP) theory.[35,52,53] The semianalytical model considers each cylinder to be an infinitely long nanowire that acts as a two-dimensional electric dipole. The incoming electric

dx.doi.org/10.1021/jp3054372 | J. Phys. Chem. C 2012, 116, 18944−18951

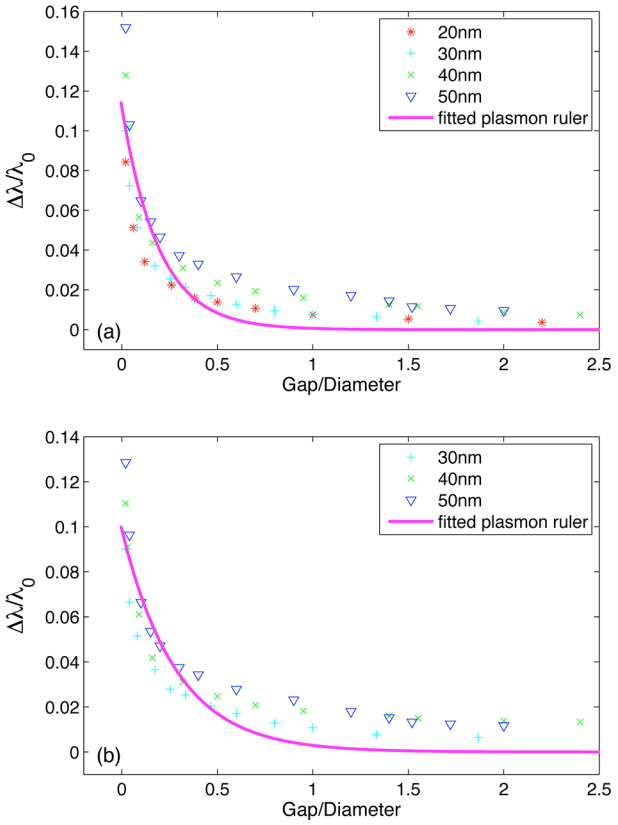

Figure 3. FDTD calculations of scaled LSPR wavelength shift vs gap distance/diameter for gold cylindrical dimers, with (a) diameters of 20−50 nm for dimers within the local model and (b) diameters of 30−50 nm for nonlocal dimers. For local dimers, we fit the results to the plasmon ruler $y = a\exp(-x/\tau)$ with 95% confidence bounds, resulting in the coupling strength $a = 0.112 \pm 0.010$ and the decay constant $\tau = 0.19 \pm 0.04$. For nonlocal dimers, the fit to the plasmon ruler results in the coupling strength $a = 0.098 \pm 0.010$ and decay constant $\tau = 0.28 \pm 0.07$.

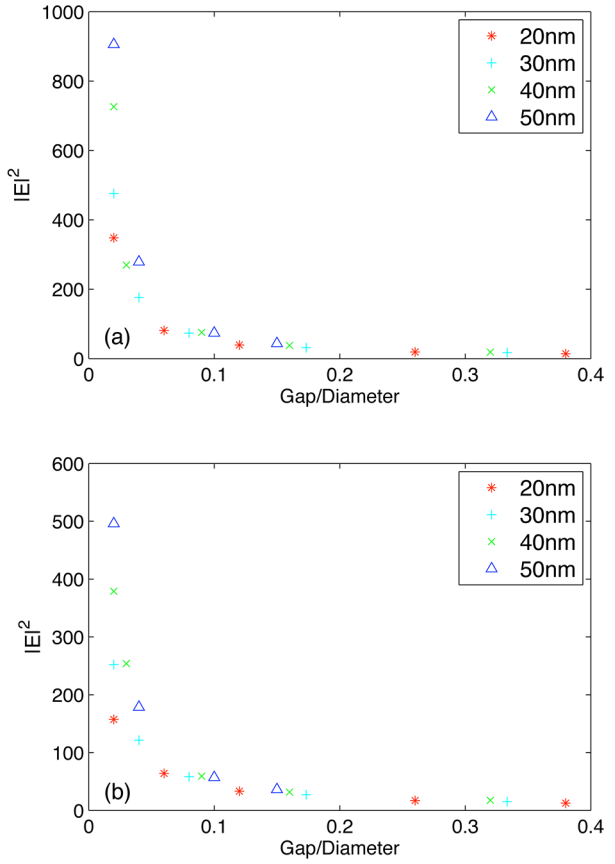

Figure 4. FDTD calculations of $|E|^2$ enhancement vs gap distance/diameter for the gold cylindrical dimers, with diameters of 20 to 50 nm for (a) local and (b) nonlocal cases. The scaled gap distance T/D varies from 0.02 to 0.4.

field is perpendicular to the cylinder axis and parallel to the dimer axis. Due to the symmetry of our dimer system, the local electric fields at equivalent positions in each cylinder are identical, and we can therefore write the electric field felt by each cylinder as the sum of the incoming field and the near-field of the neighboring electric dipole,[1,54] i.e.,

$$\mathbf{E}_{\text{local}} = \mathbf{E} + \frac{\alpha_{\text{cylinder}}}{d^2}\mathbf{E}_{\text{local}} \tag{5}$$

where, for our two-dimensional system, the near field decays as the square of the center-to-center distance d, and where, in eq 5, α_{cylinder} is the polarizability of an infinitely long cylinder. By defining $S = 1/d^2$ as the dipole sum for our dimer system and noting that S is a geometric structure factor that only depends on the relative positions of the cylinders,[2] the effective polarizability of the dimer system can be written as

$$\alpha_{\text{dimer}} = \frac{\alpha_{\text{cylinder}}}{1 - S\alpha_{\text{cylinder}}} \tag{6}$$

where

$$\alpha_{\text{cylinder}} = \frac{\varepsilon - \varepsilon_{\text{m}}}{(\varepsilon + \varepsilon_{\text{m}}) - \mathrm{i}\frac{\pi}{4}q^2(\varepsilon - \varepsilon_{\text{m}})}a^2 \tag{7}$$

and where, in eq 7, a is the cylinder radius, $q = ka$, ε_{m} is the medium dielectric constant and ε is the electric permittivity of gold. We note that, rather than using a quasistatic polarizability, we have included finite size retardation effects that become important with increasing size into the single cylinder polarizability[55,56] in eq 7. Retardation effects must be accounted for to achieve a consistent comparison with the FDTD results, since FDTD automatically accounts for retardation by meshing the cylinder cross-section. We note that the size effects $-\mathrm{i}(\pi/4)q^2(\varepsilon - \varepsilon_{\text{m}})$ due to retardation in eq 7 disappear and the dipole polarizability of a single, infinitely long metallic cylinder reduces its quasistatic counterpart $\alpha = [(\varepsilon - \varepsilon_{\text{m}})/(\varepsilon + \varepsilon_{\text{m}})]a^2$ in the limit $q \to 0$.

In the local case, because the electric permittivity depends only on frequency, we can directly apply the Drude plus Lorentz pole(s) model for gold with parameters from McMahon et al.[39] to obtain the semianalytical results. For the nonlocal case, care must be taken because we require electric permittivities that capture the nonlocal effects such that a direct relationship between the wavevector $\mathbf{k}$ and frequency ω is converted to a dependence on cylinder diameter D and wavelength λ.

We accomplish this using the effective permittivity (EP) model,[35,52,53] which is based on the electrostatic approximation and Pekar's ABC method,[39,53] and enables us to find the polarizability of small metal nanoparticles in terms of the effective permittivity $\varepsilon_{\text{L}}(D,\omega)$ based on the hydrodynamic $\varepsilon_{\text{HD}}(\mathbf{k},\boldsymbol{\omega})$ in eq 1. Here we restrict ourselves to the first order

dx.doi.org/10.1021/jp3054372 | J. Phys. Chem. C 2012, 116, 18944−18951

EP (l = 1) since only the dipolar resonance responses are utilized to construct and compare the behavior of the plasmon ruler.

By using the hydrodynamic dielectric function with EP theory to calculate the effective polarizability, we have all information necessary to not only calculate the extinction cross section of the cylindrical dimers as

$$C_{ext} = 2\pi k \, \mathrm{Im}(\alpha_{dimer}) \quad (8)$$

but also find the resonance wavelength corresponding to different separation distances for each dimer size.

To demonstrate the ability of an analytical approach to capture the observed nonlocal size effects, we first compare the local (size-independent) permittivity with the calculated EPs for different cylinder diameters taking nonlocal effects into account. As seen in Figure 5, the real parts of the nonlocal

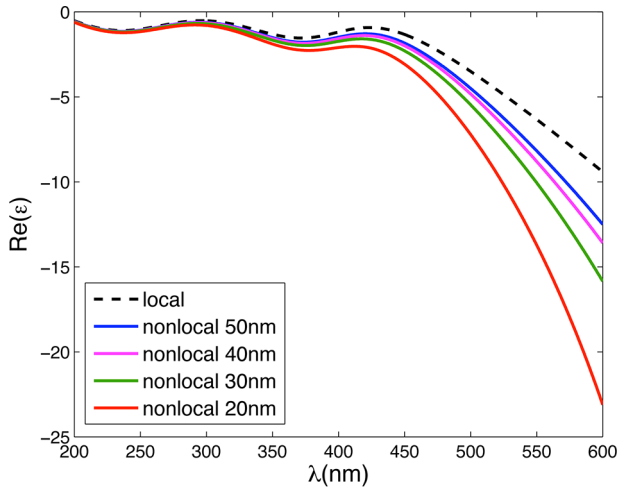

Figure 5. Effective permittivity of 20−50 nm diameter gold cylinders for local (size-independent) and nonlocal (size-dependent) material responses.

permittivities are generally smaller than the local one. This is important because the plasmon resonance requires a specific value of the real part of ε. However, as seen in Figure 5, in order to reach a specific value of the real part of ε, an increasingly strong blue shift is observed for the nonlocal cases with decreasing diameter. The results in Figure 5 also suggest a gradual increase in the importance of nonlocal effects with decreasing diameter, which may be expected to carry over to the size-dependence of the universal plasmon ruler. However, as our results in Figure 2 and Figure 3 show, while the increase in nonlocal effects is gradual, the cumulative effect to cause a deviation from the universal plasmon ruler only appears at the 20 nm diameter size scale.

In order to provide more insights into the cause for the failure of the universal plasmon ruler for the 20 nm cylinder dimers, we now employ the semianalytical theory for both local and nonlocal cases. We show the predicted universal plasmon rulers in Figure 6. It is seen that, for the local case, all cylindrical dimers with diameters ranging from 20 to 50 nm collapse upon the same curve. This result agrees with our FDTD results in Figure 3 and demonstrates that retardation, or finite size effects, are weak in this diameter range, thereby resulting in the prediction of a universal plasmon ruler.

In contrast for the nonlocal dimers as shown in Figure 6, the scaled plasmon resonance shifts $\Delta\lambda/\lambda_0$ for the 20 nm cylinder

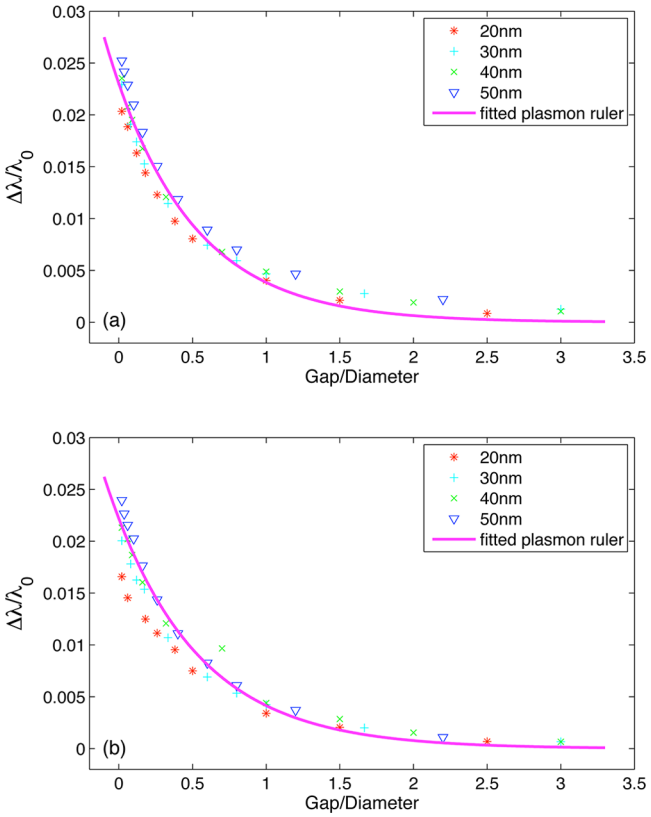

Figure 6. Semianalytical calculations of LSPR wavelength shift vs gap distance for gold cylindrical dimers, with diameters of 20 to 50 nm. (a) For local dimers, we find these follow a universal trend which can be fitted to the plasmon ruler $y = a \exp(-x/\tau)$ with the coupling strength a = 0.02299 ± 0.001 and the decay constant τ = 0.5593 ± 0.06. (b) For nonlocal dimers, the fit to the plasmon ruler results in the coupling strength a = 0.02217 ± 0.001 and decay constant τ = 0.5966 ± 0.05.

dimer deviates from the trend formed by the 30−50 nm dimers. To bring insight to the observed drop in $\Delta\lambda/\lambda_0$ for the 20 nm nonlocal dimer, we compare the value of the dipole sum S and $\mathrm{Re}(1/\alpha)$,[51] where α is the polarizability of a single cylinder with retardation, corresponding to eq 7. The reason why we are interested in these two quantities is because a more positive S leads to a stronger red shift of the LSPR wavelength, while $\mathrm{Re}(1/\alpha)$ controls the actual value of the LSPR wavelength. Here, because for all the sizes and separations $\mathrm{Re}(1/\alpha)$ is positive and larger than the dipole sum S, the LSPR wavelength shift is proportional to $1/[\mathrm{Re}(1/\alpha) - S]$, where the value of $\mathrm{Re}(1/\alpha)$ is found at the single resonance wavelength λ_0. Therefore, in order to determine the scaled plasmon resonance wavelength shifts, we divide $[\mathrm{Re}(1/\alpha) - S]$ by $\mathrm{Re}(1/\alpha)$. Hence, the values of $\Delta\lambda/\lambda_0$ follow the same trend as $\{[\mathrm{Re}(1/\alpha) - S]/[\mathrm{Re}(1/\alpha)]\}^{-1}$. Table 1 and Table 2 show these various values calculated at the smallest separation, T/D = 0.02 for both local and nonlocal material response.

We focus on the last column of both Table 1 and Table 2, which correspond to the scaled LSPR wavelength shifts (i.e., $\Delta\lambda/\lambda_0$). It is clearly seen that, for the local dimers in Table 1, the values of $\{[\mathrm{Re}(1/\alpha) - S]/[\mathrm{Re}(1/\alpha)]\}^{-1}$ for all cylinder sizes are similar, and have larger magnitudes compared to the nonlocal dimers in Table 2. This has the important implication that, for the local case, the scaled LSPR wavelength shift is independent of the dimer diameter, and instead is mainly dependent on the gap distance.

dx.doi.org/10.1021/jp3054372 | J. Phys. Chem. C 2012, 116, 18944−18951

Table 1. CDA Values for Cylindrical Dimers Assuming Local Response with Diameters Ranging from 20 to 50 nm

	local response			
diam (nm)	S	$\mathrm{Re}(1/\alpha)$	$\mathrm{Re}(1/\alpha) - S$	$\{[\mathrm{Re}(1/\alpha) - S]/[\mathrm{Re}(1/\alpha)]\}^{-1}$
20	0.002403	0.007832	0.005429	1.4426
30	0.001068	0.003483	0.002415	1.4422
40	0.000601	0.001955	0.001354	1.4435
50	0.000384	0.001248	0.000864	1.4452

Table 2. CDA Values for Cylindrical Dimers Assuming Nonlocal Response with Diameters Ranging from 20 to 50 nm

	nonlocal response			
diam (nm)	S	$\mathrm{Re}(1/\alpha)$	$\mathrm{Re}(1/\alpha) - S$	$\{[\mathrm{Re}(1/\alpha) - S]/[\mathrm{Re}(1/\alpha)]\}^{-1}$
20	0.002403	0.008995	0.006592	1.3645
30	0.001068	0.003859	0.002808	1.3827
40	0.000601	0.002133	0.001532	1.3921
50	0.000384	0.001343	0.000959	1.4011

However, when we include nonlocality by replacing the size-independent local permittivity by EP, the values of $\{[\mathrm{Re}(1/\alpha) - S]/[\mathrm{Re}(1/\alpha)]\}^{-1}$ in Table 2 decrease with decreasing size, with a large variation in going from the 30 to 20 nm diameter, similar to what was observed for the effective permittivity in Figure 5, which explains why we observe in both the FDTD and semianalytical results the size-dependent deviation from the universal plasmon ruler starting from the 20 nm diameter. Furthermore, this shows directly that the size dependence of the plasmon ruler for small dimer sizes cannot be reflected using the local model.

A physical explanation for the observed size dependence due to nonlocal effects can be obtained by delineating between surface and volume plasmons. We emphasize that this explanation was initially proposed by McMahon et al.[39,40] for nanoparticle dimers by noting the excitement of volume plasmons by the wavevector **k**, in which a larger **k** requires a higher frequency to induce the plasmon resonance. In the present work, we utilize the same concept of volume plasmons to explain the nonlocal effects, though with a slightly different physical origin.[57]

For a purely local theory, the induced charge rests at the surface of the cylinder, and does not extend into the bulk.[57] Furthermore, the electric field strength decays exponentially in going from the cylinder−air interface into the bulk, which is also driven by surface plasmons. However, in nonlocal theory, electrons in the conduction band do not behave as a purely free electron gas. Consequently, the induced charge exists not only at the surface but also inside the cylinder which leads to volume plasmons. The internal electric field then is composed of two exponentially decaying fields,[57] one due to surface plasmons as described by the local theory, and the other one due to volume plasmons, which can be captured with the nonlocal hydrodynamic dielectric function. Hence the internal electric field that is bound to the cylinder surface is modified through the coupling between surface and volume plasmons, which in turn alters the plasmon resonance condition. Because the induced charge is not entirely confined at the surface, nonlocal effects soften or screen the short distance interactions of the induced charge at the gap, which leads to a larger effective gap distance,[38,58] and is the reason why using nonlocal theory a blue-shifted LSPR wavelength is observed as compared to the local case.

For the larger diameter cylinders, the relative contribution of volume plasmons to the total electric field is minimal, because it is the evanescent field of the volume plasmons that couples to surface plasmons and modifies the internal electric field, and thus the relative contribution of the volume plasmons to the total electric field is only important close to the surface of the cylinder. Therefore, for the large diameter dimers little deviation from the local results is observed[42] and the universal plasmon ruler is obeyed. However, for the smallest (20 nm diameter) dimers, higher wave vectors are generated for each gap separation, so nonlocal effects become more important with the excitation of the volume plasmons. Furthermore, the effective area of the cylinders where the effects of volume plasmons are important increases,[42] which enhances the importance of nonlocal effects, and contributes to the deviation of 20 nm diameter nonlocal dimer from the universal plasmon ruler.

CONCLUSIONS

We have utilized a combination of FDTD numerical calculations and semianalytical models based upon the coupled dipole approximation to study the validity of the universal plasmon ruler[1] for a wide range of nanocylinder dimer diameters. We found that, if nonlocal effects are accounted for, which are important for very small gap distances between nanoparticles, dimers with diameters smaller than about 20 nm do not follow the universal plasmon ruler. The present results, when coupled with previous results[2] showing a dynamic depolarization-induced finite size-dependence for larger diameter dimers, establish a validity range for the universal plasmon ruler: 20 nm diameter dimers at the lower end, and 70 nm diameter dimers at the upper end.

APPENDIX

For the nonlocal FDTD simulations, the equations that update the currents **J** corresponding to the Lorentz term $\varepsilon_{\mathrm{Lorentz}}$ in $\varepsilon(\mathbf{k},\omega)$ remain the same as in the local formulation because the Lorentz terms involve only ω and ω^2, which result in standard first and second derivatives in time.

However, because the hydrodynamic Drude term $\varepsilon_{\mathrm{HD}}(\mathbf{k},\omega)$ has a wavevector dependence through the $-\beta\mathbf{k}^2$ term in eq 1, the currents corresponding to the Drude term result in an additional second order derivative in space. It is clear that $\varepsilon_{\mathrm{HD}}$ differs from the standard Drude dielectric function through incorporation of the wavevector **k**, which accounts for the spatial dispersion through the nonlocal effects. This implies that the bound, or core, electrons, which are typically modeled using Lorentz terms, are left in local form in the present work. A similar approximation has previously been utilized by Garcia de Abajo[38] and McMahon et al.[39] in theoretical studies of nonlocal effects on the optical properties of small metal nanostructures.

We show herein the three fundamental update equations for the electric and magnetic fields and also the induced currents related to the dielectric response of metal, while referring readers to McMahon et al.[39] for more details on the standard FDTD equations:

dx.doi.org/10.1021/jp3054372 | J. Phys. Chem. C 2012, 116, 18944−18951

$$\frac{\partial^2}{\partial t^2}\mathbf{J}_L(\mathbf{x}, t) + 2\delta_L\frac{\partial}{\partial t}\mathbf{J}_L(\mathbf{x}, t) + {\omega_L}^2\mathbf{J}_L(\mathbf{x}, t) = \varepsilon_0\Delta\varepsilon_L{\omega_L}^2\frac{\partial}{\partial t}\mathbf{E}(\mathbf{x}, t)$$

$$\frac{\partial^2}{\partial t^2}\mathbf{J}_{HD}(\mathbf{x}, t) + \gamma\frac{\partial}{\partial t}\mathbf{J}_{HD}(\mathbf{x}, t) - \beta^2\nabla^2\mathbf{J}_{HD}(\mathbf{x}, t) = \varepsilon_0{\omega_D}^2\frac{\partial}{\partial t}\mathbf{E}(\mathbf{x}, t)$$

$$\varepsilon_0\varepsilon_\infty\frac{\partial}{\partial t}\mathbf{E}(\mathbf{x}, t) + \mathbf{J}_L(\mathbf{x}, t) + \mathbf{J}_{HD}(\mathbf{x}, t) = \nabla \times \mathbf{H}(\mathbf{x}, t) \quad (9)$$

From the above eq 9, we see that, through the FDTD algorithm, the essence of nonlocal effects on the optical properties of metal nanostructures is clearly illustrated. Specifically, we see in eq 9 that, because of the $-\beta^2\nabla^2\mathbf{J}_{HD}(\mathbf{x},t)$ term, the current density at a given point in space is related not only to the field at the same point but also to the field at previous time steps at neighboring points, which results in a dependence on both $\boldsymbol{\omega}$ and $\mathbf{k}$.

It is also worth noting that, in our FDTD implementation including nonlocal effects, the update algorithm is based on the assumption that the curl of the Drude current is zero, and that both the normal and tangential parts of the Drude currents vanish at the boundary, which corresponds to Pekar's additional boundary condition (ABC).[39,53] However, Raza et al.[59] have recently found that care should be taken when applying Pekar's ABC, as it may introduce nonphysical ripples on the main extinction peak. In the hydrodynamic Drude model, the tangential part of the Drude current need not be zero at the boundary, since we are assuming a nonviscous material. Thus, even though Pekar's ABC produces unwanted ripples, it predicts a similar plasmon dipolar resonance shift as compared to the full hydrodynamic model as shown by Raza et al.,[59] and thus we utilize this approach to study the plasmon resonance wavelength shift as the distance between nanoparticles decreases.

AUTHOR INFORMATION

Corresponding Author

*E-mail: parkhs@bu.edu.

Notes

The authors declare no competing financial interest.

ACKNOWLEDGMENTS

H.S.P. and X.B. both gratefully acknowledge NSF Grant No. CMMI-1036460 in support of this research. X.B. also acknowledges helpful discussions with Dr. Jeffrey McMahon about his local FDTD code and nonlocal algorithm.[39]

REFERENCES

(1) Jain, P. K.; Huang, W.; El-Sayed, M. A. *Nano Lett.* **2007**, *7*, 2080−2088.
(2) Ben, X.; Park, H. S. *J. Phys. Chem. C* **2011**, *115*, 15915−15926.
(3) Ozbay, E. *Science* **2006**, *311*, 189−193.
(4) Sambles, J. R.; Bradbery, G. W.; Yang, F. *Contemp. Phys.* **1991**, *32*, 173−183.
(5) Barnes, W. L.; Dereux, A.; Ebbeson, T. W. *Nature* **2003**, *424*, 824−830.
(6) Nie, S.; Emory, S. R. *Science* **1997**, *275*, 1102−1106.
(7) Hao, E.; Schatz, G. C. *J. Chem. Phys.* **2004**, *120*, 357−366.
(8) Kneipp, K.; Moskovits, M.; Kneipp, H. E. *Surface-Enhanced Raman Scattering*; Springer: 2006.
(9) Kelly, K. L.; Coronado, E.; Zhao, L. L.; Schatz, G. C. *J. Phys. Chem. B* **2003**, *107*, 668−677.
(10) Link, S.; El-Sayed, M. A. *J. Phys. Chem. B* **1999**, *103*, 8410−8426.
(11) Lee, K.-S.; El-Sayed, M. A. *J. Phys. Chem. B* **2005**, *109*, 20331−20338.
(12) Raschke, G.; Brogl, S.; Susha, A. S.; Rogach, A. L.; Klar, T. A.; Feldmann, J.; Fieres, B.; Petkov, N.; Bein, T.; Nichtl, A.; Kurzinger, K. *Nano Lett.* **2004**, *4*, 1853−1857.
(13) Sokolov, K.; Follen, M.; Aaron, J.; Pavlova, I.; Malpica, A.; Lotan, R.; Richards-Kortum, R. *Cancer Res.* **2003**, *63*, 1999−2004.
(14) El-Sayed, I. H.; Huang, X.; El-Sayed, M. A. *Nano Lett.* **2005**, *5*, 829−834.
(15) Mock, J. J.; Oldenburg, S. J.; Smith, D. R.; Schultz, D. A.; Schultz, S. *Nano Lett.* **2002**, *2*, 465−469.
(16) Anker, J. N.; Hall, W. P.; Lyandres, O.; Shah, N. C.; Zhao, J.; Duyne, R. P. V. *Nat. Mater.* **2008**, *7*, 442−453.
(17) Hirsch, L. R.; Stafford, R. J.; Bankson, J. A.; Sershen, S. R.; Rivera, B.; Price, R. E.; Hazle, J. D.; Halas, N. J.; West, J. L. *Proc. Natl. Acad. Sci. U.S.A.* **2003**, *100*, 13549−13554.
(18) Hirsch, L. R.; Gobin, A. M.; Lowery, A. R.; Tam, F.; Drezek, R. A.; Halas, N. J.; West, J. L. *Ann. Biomed. Eng.* **2006**, *34*, 15−22.
(19) Huang, X.; El-Sayed, I. H.; Qian, W.; El-Sayed, M. A. *J. Am. Chem. Soc.* **2006**, *128*, 2115−2120.
(20) Acimovic, S. S.; Kreuzer, M. P.; Gonzales, M. U.; Quidant, R. *ACS Nano* **2009**, *3*, 1231−1237.
(21) Atay, T.; Song, J.-H.; Nurmikko, A. V. *Nano Lett.* **2004**, *4*, 1627−1631.
(22) Aizpurua, J.; Bryant, G. W.; Richter, L. J.; de Abajo, F. J. G.; Kelley, B. K.; Mallouk, T. *Phys. Rev. B* **2005**, *71*, 235420.
(23) Oubre, C.; Nordlander, P. *J. Phys. Chem. B* **2005**, *109*, 10042−10051.
(24) Rechberger, W.; Hohenau, A.; Leitner, A.; Krenn, J. R.; Lamprecht, B.; Aussenegg, F. R. *Opt. Commun.* **2003**, *220*, 137−141.
(25) Romero, I.; Aizpurua, J.; Bryant, G. W.; de Abajo, F. J. G. *Opt. Express* **2006**, *14*, 9988−9999.
(26) Su, K.-H.; Wei, Q.-H.; Zhang, X.; Mock, J. J.; Smith, D. R.; Schultz, S. *Nano Lett.* **2003**, *3*, 1087−1090.
(27) Talley, C. E.; Jackson, J. B.; Oubre, C.; Grady, N. K.; Hollars, C. W.; Lane, S. M.; Huser, T. R.; Nordlander, P.; Halas, N. J. *Nano Lett.* **2005**, *5*, 1569−1574.
(28) Xu, H.; Kall, M. *Phys. Rev. Lett.* **2002**, *89*, 246802.
(29) Willets, K. A.; Duyne, R. P. V. *Annu. Rev. Phys. Chem.* **2007**, *58*, 267−297.
(30) Alexander, K. D.; Skinner, K.; Zhang, S.; Wei, H.; Lopez, R. *Nano Lett.* **2010**, *10*, 4488−4493.
(31) Xu, H.; Aizpurua, J.; Kall, M.; Apell, P. *Phys. Rev. E* **2000**, *62*, 4318−4324.
(32) Kneipp, K.; Wang, Y.; Kneipp, H.; Perelman, L. T.; Itzkan, I.; Dasari, R. R.; Feld, M. S. *Phys. Rev. Lett.* **1997**, *78*, 1667−1670.
(33) Sonnichsen, C.; Reinhard, B. M.; Liphardt, J.; Alivisatos, A. P. *Nat. Biotechnol.* **2005**, *23*, 741−745.
(34) Reinhard, B. M.; Siu, M.; Agarwal, H.; Alivisatos, A. P.; Liphardt, J. *Phys. Rev. B* **2005**, *76*, 085420.
(35) Fuchs, R.; Claro, F. *Phys. Rev. B* **1987**, *35*, 3722−3727.
(36) Jones, W. E.; Kliewer, K. L.; Fuchs, R. *Phys. Rev.* **1969**, *178*, 1201−1203.
(37) McMahon, J. M.; Gray, S. K.; Schatz, G. C. *Phys. Rev. Lett.* **2009**, *103*, 097403.
(38) de Abajo, F. J. G. *J. Phys. Chem. C* **2008**, *112*, 17983−17987.
(39) McMahon, J. M.; Gray, S. K.; Schatz, G. C. *Phys. Rev. B* **2010**, *82*, 035423.
(40) McMahon, J. M.; Gray, S. K.; Schatz, G. C. *Nano Lett.* **2010**, *10*, 3473−3481.
(41) David, C.; de Abajo, F. J. G. *J. Phys. Chem. C* **2011**, *115*, 19470−19475.
(42) Yannopapas, V. *J. Phys.: Condens. Matter* **2008**, *20*, 325211.

(43) Pack, A.; Hietschold, M.; Wannemacher, R. *Opt. Commun.* **2001**, *194*, 277−287.
(44) Palomba, S.; Novotny, L.; Palmer, R. E. *Opt. Commun.* **2008**, *281*, 480−483.
(45) Yang, Y.; Wang, H.; Yan, B.; Reinhard, B. M. *J. Phys. Chem. C* **2010**, *114*, 4901−4908.
(46) Bohren, C. F.; Huffman, D. R. *Absorption and scattering of light by small particles*; Wiley-Interscience: 1983.
(47) Toscano, G.; Wubs, M.; Xiao, S.; Yan, M.; Öztürk, Z.; Jauho, A.; Mortensen, N. *Proc. SPIE* **2010**, *7757*, 77571T.
(48) Boardman, A. *Electromagnetic surface modes*; Wiley: 1982.
(49) Taflove, A.; Hagness, S. *Computational electrodynamics*; Artech House: Boston, 1995.
(50) Coronado, E. A.; Schatz, G. C. *J. Chem. Phys.* **2003**, *119*, 3926−3934.
(51) Zhao, L.; Kelly, K. L.; Schatz, G. C. *J. Phys. Chem. B* **2003**, *107*, 7343−7350.
(52) Dasgupta, B.; Fuchs, R. *Phys. Rev. B* **1981**, *24*, 554.
(53) Ruppin, R. *J. Opt. Soc. Am. B* **1989**, *6*, 1559−1563.
(54) Novotny, L.; Hecht, B. *Principles of nano-optics*; Cambridge University Press: 2006.
(55) Meier, M.; Wokaun, A. *Opt. Lett.* **1983**, *8*, 581−583.
(56) Gómez-Medina, R.; Laroche, M.; Sáenz, J. *Opt. Express* **2006**, *14*, 3730−3737.
(57) Fuchs, R.; Kliewer, K. L. *Phys. Rev. B* **1971**, *3*, 2270−2278.
(58) Jacak, J.; Krasnyj, J.; Jacak, W.; Gonczarek, R.; Chepok, A.; Jacak, L. *Phys. Rev. B* **2010**, *82*, 035418.
(59) Raza, S.; Toscano, G.; Jauho, A.-P.; Wubs, M.; Mortensen, N. A. *Phys. Rev. B* **2011**, *84*, 121412(R).